Trip length estimation for the macroscopic traffic simulation: scaling microscopic into macroscopic networks

S. F. A. Batista *
Univ. Lyon, ENTPE, IFSTTAR, LICIT
UMR _T 9401, F-69518, LYON, France
Tel: +33 4 72 04 71 65
Email: sergiofilipe.assuncaobatista@entpe.fr

and

Urban Transport Systems Laboratory
School of Architecture, Civil and Environmental Engineering École Polytechnique Fédérale de Lausanne, Switzerland

Ludovic Leclercq
Univ. Lyon, ENTPE, IFSTTAR, LICIT
UMR _T 9401, F-69518, LYON, France
Tel: +33 4 72 04 77 16
Email: ludovic.leclercq@entpe.fr

Jean Krug
Univ. Lyon, ENTPE, IFSTTAR, LICIT
UMR _T 9401, F-69518, LYON, France
Tel: +33 4 72 04 70 64
Email: jean.krug@entpe.fr

Nikolas Geroliminis
Urban Transport Systems Laboratory
School of Architecture, Civil and Environmental Engineering École Polytechnique Fédérale de Lausanne, Switzerland
Tel: +41 (21) 693-2481
Email: nikolas.geroliminis@epfl.ch

* Corresponding author

Paper submitted for presentation at the 97th Annual Meeting Transportation Research Board, Washington D.C., January 2018

Special call by AHB45 committee on “Advances in modeling and traffic management for large-scale urban network”

1 Word count: 4827 words + 5 figure(s) $\times$ 250 + 3 table(s) $\times$ 250 + 500 (references) = 7327 words

2 August 1, 2017

ABSTRACT

After the seminal works of Daganzo (*1*) and Geroliminis and Daganzo (*2*), the traffic simulation based on the Macroscopic Fundamental Diagram (MFD) has been gaining more and more interest from the scientific community, especially in applications for control purposes. One fundamental question for this type of simulation is the proper definition of the macroscopic trip lengths. Some approaches have been discussed in the literature (Daganzo, Yildirimoglu and Geroliminis, Ramezani et al., *1, 3, 4*). However, no study focus on the definition of the macroscopic trip lengths based on the microscopic network.

In this paper, we discuss three methods to calculate the macroscopic trip lengths based on the aggregation of microscopic trips, within each reservoir considering: (i) no further information; (ii) the next reservoir to be traveled; and (iii) the related macro-path (i.e., the list of reservoirs that are crossed from the Origin to the Destination). Based on a static analysis of the network, we show that these methods: yield different average trip lengths at the reservoir level; and give similar average trip lengths at the macroscopic-path level, where the aggregation effect is on the standard deviation. We analyze the dependence of the trip lengths on the Origin-Destination matrix. We discuss a procedure to estimate the macroscopic trip lengths based on a new Origin-Destination matrix. We show that the estimated trip lengths show a good agreement with the ones calculated based on a new calculation of the microscopic trips, for the new Origin-Destination matrix. We analyze the impact of the macroscopic trip lengths on the traffic states, that are simulated using an accumulation-based simulator. We show that the trip lengths have a strong impact on the traffic states. And, the trip lengths are congestion-dependent when calculated at the reservoir level.

Keywords: Macroscopic Trip Lengths, Accumulation-based Macroscopic Simulation, Macroscopic Fundamental Diagram, Congestion, MFD Dynamics

INTRODUCTION

The first ideas of macroscopic traffic simulation based on the decomposition of a city into reservoirs were introduced by Godfrey (*5*). But, it really started attracting more attention from the scientific community after the seminal works of Daganzo (*1*) and Geroliminis and Daganzo (*2*). Each reservoir is defined by a well-defined relation between mean flow and accumulation, the Macroscopic Fundamental Diagram (MFD). Based on Yokohama (Japan) traffic data, Geroliminis and Daganzo (*2*) provided ground truth evidence of the MFD existence. This has been confirmed by further studies: e.g., Buisson and Ladier, Ambühl and Menendez, Derrman et al., Lodera et al. (*6, 7, 8, 9*). The applications of the MFD in simulation has mostly been for now for testing different control algorithms: Haddad and Geroliminis (*10*); Ekbatani et al. (*11*); Ramezani et al. (*4*); and Haddad (*12*), for some examples.

The mathematical formulation of the MFD was introduced by Daganzo (*1*), for a single reservoir. The traffic dynamics is governed by a state equation that relates the vehicle's accumulation ($n(t)$) with the balance between the inflow ($f(t)$) and outflow ($g(t)$). Depending on the assumption made on $g(t)$, one can distinguish two models in the literature: the accumulation-based model (Daganzo, Geroliminis and Daganzo, *1, 2*); and the trip-based model (Arnott, *13*). One main difference between both models lies in the definition of the trip lengths for a macroscopic path (macro-path). A macro-path is defined as a sequence of reservoirs in a multi-region network level approach.

The first implementation of the accumulation-based model assumes a constant mean trip length ($\bar{L}$) for all vehicles traveling inside the same reservoir (Daganzo, *1*). This assumption might not be realistic in cases where the mean trip lengths are highly influenced by origins and destinations (Leclercq et al., *14*). While, empirical results in Yokohama showed that this might be a reasonable assumption for a range of cases. Yildirimoglu and Geroliminis (*3*) proposes different average trip lengths for the different macro-paths crossing the same reservoir. The same work also proposes to split the conservation equation into different classes of vehicles that share a common travel distance. Ramezani et al. (*4*) proposes a more refined approach, where the trip lengths are dynamically calculated. The trip lengths are calculated for all vehicles traveling on reservoir i and going to a common adjacent reservoir j, depending on the exchange flows and accumulation. An accumulation-based model considers that the network outflow depends on the average trip length (without specifying in details which type of average is taken).

A trip-based model (Arnott, Fosgerau, Lamotte and Geroliminis, Leclercq et al., Mariotte et al., *13, 15, 16, 17, 18*) emphasizes that the outflow depends on the rate at which vehicles complete a generating trip length in the beginning of the trip and keeps track of the distance traveled for each vehicle. Recent work (Lamotte and Geroliminis, Mariotte et al., *16, 18*) showed that hysteresis loops might be generated in the outflow MFD between the onset and offset of congestion, even if the production MFD has no hysteresis.

Both accumulation- and trip-based approaches thus require a proper estimation of trip lengths within reservoirs. On the other hand, a definition of the trip lengths at the macro-path level is required for the first traffic assignment iteration. Thus, dedicated methods able to scale up trips from the real (microscopic) network to the reservoirs (macroscopic) network should be designed and validated. These methods should be able to easily calculate trip lengths at the reservoir and at the macro-path levels.

In this paper, we propose to investigate three methods to calculate macroscopic trip lengths. The idea is to use the microscopic network to generate individual trips and then aggregate them

within the reservoirs considering: (i) no further information; (ii) the next reservoir to be traveled (i.e., the adjacent destination reservoir); and (iii) the related macro-path. These methods allow to obtain a trip length distribution at the reservoir level. The calculation of the trip lengths at the macro-path level is directly obtained by averaging the means of the trip length distribution over the sequence of reservoirs crossed. We note that these methods can be directly applied to both the accumulation- and trip-based models. We test these aggregation methods on the 6^{th} Lyon district network (France), that is divided into eight reservoirs. We analyze the differences in the distributions of trip lengths obtained through the three methods. We then discuss an approach to estimate the macroscopic trip lengths, considering the Origin-Destination (OD[1]) matrix between reservoirs without requiring the re-sampling of micro-trips. Finally, we test the three calculation methods by performing an accumulation-based dynamic simulations, considering the Wardrop equilibrium on the macro-paths. Finally, we show that the calculation methods highly influences the simulation results and the network equilibrium. We show that trip lengths are sensible to congestion at the reservoir level.

[1]Capital letters refer to macroscopic OD's, while lower case letters refer to microscopic od's.

THEORETICAL BACKGROUND ON THE ACCUMULATION-BASED MACROSCOPIC SIMULATION

The traffic dynamics inside a single reservoir is governed by the evolution of the accumulation (*n(t)*):

$$\frac{dn}{dt} = f(t) - g(t) \tag{1}$$

where *f(t)* is the inflow function and *g(t)* is the outflow function.

Daganzo (*1*) proposes that the outflow function (*g(t)*) depends on *n(t)*; and is proportional to the average trip length $\bar{L}$:

$$g(t) \approx \frac{P(n(t))}{\bar{L}} \tag{2}$$

where $P(n(t))$ is the travel production that depends on the accumulation $n(t)$.

Daganzo (*1*) proposes to consider an average trip length $\bar{L}$ for all vehicles traveling on the same reservoir. Some authors also consider an average trip length at the reservoir level and independent of the OD, for: a macroscopic simulator set-up (Daganzo, Ramezani et al., Gayah and Dagamzo, *1, 4, 19*); control purposes (see e.g., Haddad, *12*).

Yildirimoglu and Geroliminis (*3*) and Ramezani et al. (*4*) propose more refined approaches for the definition of the trip lengths. Yildirimoglu and Geroliminis (*3*) proposes an average trip length for all vehicles traveling on the same reservoir and on the same macro-path. Ramezani et al. (*4*) proposes a dynamic calculation of the trip lengths that depend on the accumulation $n_i(t)$ inside reservoir i and on the MFD dynamics. The authors separate internal from other trips going to the adjacent reservoirs:

$$L_i(t) = \frac{P(n_i(t))}{q_i(t)} \tag{3}$$

$$L_{ij}(t) = \frac{n_{ij}(t)}{n_i(t)} \frac{P(n_i(t))}{q_{ij}(t)} \tag{4}$$

where Eq. 3 is valid for internal trips (or internal trip endings) to reservoir i; and Eq. 4 is valid for the trips going to the adjacent reservoirs. $L_i(t)$ is the internal trip length for reservoir i. $q_i(t)$ is the internal flow on reservoir i. $n_{ij}(t)$ is the accumulation that goes from reservoir i to the adjacent reservoir j. $q_{ij}(t)$ is the transfer flow between reservoirs i and j.

TRIP LENGTH DISTRIBUTIONS: METHODOLOGICAL FRAMEWORK

In this section, we describe the proposed methods to calculate the trip lengths. We start from the microscopic network and perform a uniform sampling of N_{trips} od pairs. For each od pair, we calculate effective micro-trips using the Dijkstra algorithm. Micro-trips represent shortest-paths between the od pairs. Let Γ be the set of the calculated micro-trips. We describe now three methods to aggregate micro-trips and calculate macroscopic trip lengths. We present the mathematical formulation of these methods at: (i) the reservoir level that is crucial for the macroscopic simulation; and (ii) the macro-path level that is important for the first assignment iteration.

At the reservoir level, these methods are defined as:

1. *Method 1: no information.* All micro-trips that travel on the $i-$th reservoir are aggregated to calculate the average trip length $\bar{L_i}$ of reservoir i:

$$\bar{L_i} = \frac{\sum_k l_i^k}{\sum_k \delta_{ik}}, \forall k \in \Gamma \tag{5}$$

   where l_i^k is the portion of micro-trip k that belongs to reservoir i; and δ_{ik} is a dummy variable that equals 1 if micro-trip k travels on reservoir i.

   The set of trip lengths of reservoir i is:

$$L_i = \{l_i^k\}, \forall k \in \Gamma \tag{6}$$

2. *Method 2: next destination adjacent reservoir.* All micro-trips traveling on the $i-$th reservoir and going to the $j-$th adjacent reservoir are aggregated to define the average trip length $\bar{L_{ij}}$ to go from reservoir i to j:

$$\bar{L_{ij}} = \frac{\sum_k \delta_{ijk} l_i^k}{\sum_k \delta_{ijk}}, \forall k \in \Gamma \wedge \forall j \in \Lambda \tag{7}$$

   where δ_{ijk} is a dummy variable that equals 1 if micro-trip k travels on reservoir i and goes to reservoir j; and Λ is the set of adjacent reservoirs to i.

   The set of trip lengths of reservoir i that goes to j is:

$$L_{ij} = \{\delta_{ijk} l_i^k\}, \forall k \in \Gamma \tag{8}$$

3. *Method 3: related macro-path p.* All micro-trips that travel on reservoir i and both belong to macro-path p are aggregated to define the average trip length of p on reservoir i ($\bar{L_i^p}$):

$$\bar{L_i^p} = \frac{\sum_k \delta_{ik}^p l_i^k}{\sum_k \delta_{ik}^p}, \forall k \in \Gamma \tag{9}$$

   where δ_{ik}^p is a dummy variable that equals 1 if micro-trip k travels on reservoir i and both define macro-path p.

The set of trip lengths for macro-path p on reservoir i is:

$$L_i^p = \{\delta_{ik}^p l_i^k\}, \forall k \in \Gamma \tag{10}$$

Consider that macro-path p is defined as the following sequence of reservoirs:

$$p = (p_1, \dots p_m, \dots, p_R), \forall m = 1, \dots, R \tag{11}$$

where R is the number of reservoirs that define p.

The average trip lengths at the macro-path level (L_p) are directly calculated from the previous definitions at the reservoir level:

1. *Method 1:*

$$\bar{L_p} = \sum_{m=p_1}^{p_R} \bar{L_m} \tag{12}$$

2. *Method 2:*

$$\bar{L_p} = \sum_{m=p_1}^{p_R} \sum_{l=p_{m+1}}^{p_{R-1}} \bar{L_{ml}} + \bar{L_{p_R p_R}} \tag{13}$$

3. *Method 3:*

$$\bar{L_p} = \sum_{m=p_1}^{p_R} \bar{L_m^p} \tag{14}$$

At the macro-path level, the variances of L_p are calculated through the convolution of the variances of the set of trip lengths of the R reservoirs that define p. This means that we assume independent trip length distributions at the reservoir level.

Note that, the set of the trip lengths previously defined at the reservoir level strongly depend on the algorithm used to calculate the micro-trips. For now, we focus on shortest-paths in distance over the microscopic network. More refined approaches like Frejinger et al. (*20*) and Flotterod and Bierlaire (*21*) will be investigated in future research.

There are also other factors that may play an important role. Leclercq et al. (*14*) shows that (i) traffic conditions and (ii) od matrix influence the trip lengths. The (iii) value of N_{trips} and (iv) the definition of a macro-path are other important factors. Points (iii) and (iv) will be subject to future research, while points (i) and (ii) will be investigated in this study.

STATIC ANALYSIS OF THE MACROSCOPIC TRIP LENGTHS

Network definition

To test the proposed methods to calculate the trip length distributions, we consider the Lyon 6^{th} district network shown in Fig. 1. This network has 757 links, 431 nodes and arbitrarily divided into 8 reservoirs.

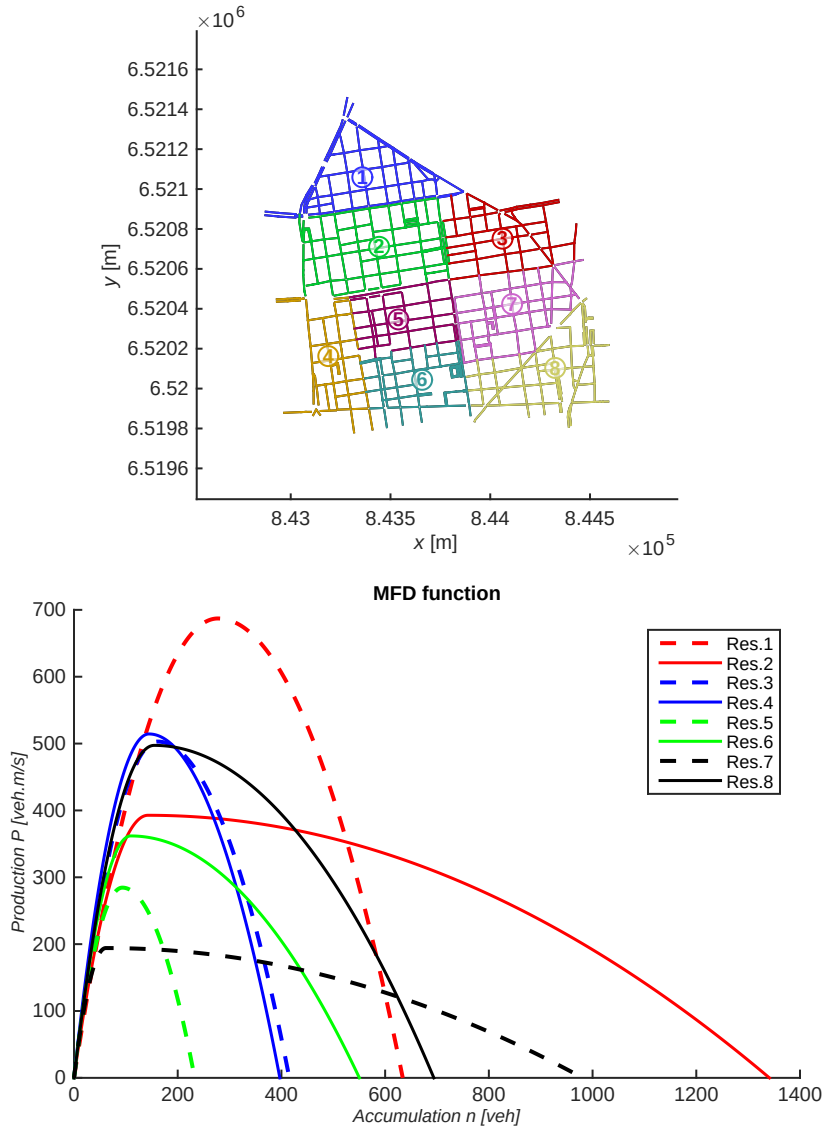

FIGURE 1 : *Top:* Lyon 6^{th} district network divided into 8 reservoirs. *Bottom:* MFD function of each reservoir.

The MFD functions (Fig. 1) are determined using a microscopic simulator called Symuvia (Leclercq, *22*). We consider a larger network that incorporates the 3^{rd} and 6^{th} districts of Lyon and the neighbor city of Villeurbarnne. This network covers a surface of 40 square kilometers. We consider two types of demand: a static demand that consists of $\sim$ 800.000 vehicles and is estimated using the model of Cabrera Delgado and Bonnel (*23*); and a dynamic demand that is obtained by

combining daily demand and loop detectors measurements. We consider MFD sensors placed on the larger network and the data is aggregated every 10 minutes. We assume a bi-parabolic shape to fit the simulated data.

We sample $N_{trips} = 10000$ od pairs and calculate the micro-trips. We exclude the micro-trips that cross more than one time the same reservoir and we are left with ~ 9200 micro-trips, that define 205 macro-paths. We hereafter refer to this set of macro-paths as Ψ and the corresponding set of micro-trips as Ξ. The aggregation of the od pairs into the OD matrix is listed in Table 1. We refer to this OD matrix as M. In this static analysis, we also have interest to investigate the impact of the OD matrix on the trip lengths. For this, we consider a second arbitrary sampling of $N_{trips} = 10000$ od pairs, where there are more od pairs samples on the origin reservoir 1 and destination reservoirs 4, 6 and 8. This means, we are considering more micro-trips that go from the north to the south of the network (i.e., from reservoir 1 to 4, 6 and 8). For each of the previous OD, we sample 600 od pairs, out of the 10000. The remaining od pairs are uniformly sampled on the microscopic network. We refer to this second OD matrix as M^* and the results are listed in Table 1. We consider M^* to investigate the influence of the OD matrix on the trip lengths; and to introduce a procedure to calibrate the trip lengths based on the OD matrices information, without the need to recalculate the micro-trips.

Destination reservoir

Origin Reservoir	1	2	3	4	5	6	7	8
1	171	204	125	141	96	147	120	163
2	210	294	202	189	149	214	190	270
3	196	245	121	141	87	103	115	174
4	146	214	113	110	87	128	111	170
5	87	160	66	88	67	109	92	126
6	134	154	109	79	82	80	129	147
7	124	201	120	88	89	72	106	139
8	211	227	161	156	85	118	181	187

Destination reservoir

Origin Reservoir	1	2	3	4	5	6	7	8
1	171	204	125	141	96	147	120	163
2	145	250	85	589	125	589	133	572
3	199	276	175	207	110	249	174	333
4	144	181	72	110	77	108	87	148
5	86	102	49	77	48	83	76	119
6	105	136	78	66	56	52	100	116
7	141	122	79	77	67	48	93	149
8	181	202	140	113	71	130	123	135

TABLE 1 : Number of trips between each macroscopic origin and destination reservoirs, for the 6^{th} Lyon district network. *Top:* Matrix M. *Bottom:* Matrix M^*.

Analysis of the trip length distributions

We first consider the aggregation of the micro-trips by reservoir. In Fig. 2, we show the average trip length for the aggregation methods 1 and 2. For method 3, we show the histogram of trip lengths of all macro-paths that cross a reservoir. As observed in Fig. 2, it is clear that the destination and the specific macro-paths matter as the trip lengths are different than the mean of method 1, when we segment the micro-trips at the reservoir level. In fact, as shown by Leclercq et al. (*14*), the hypothesis of method 1 is clearly a strong restriction for MFD simulation. This will be investigated in the next section.

We now investigate the impact of the three methods at the macro-path level. For this, we consider all possible OD pairs and the most sampled macro-path for each OD (i.e., the macro-paths that have the largest number of aggregated micro-trips, at the macro-path level). We show that the impact of the different aggregation methods is on the macroscopic trip length standard deviations and not on the averages. The averages are approximately similar for the three methods and the different OD's. But there are some exceptions, such as for the following OD's: 2-8; 3-8; 5-8; 8-1; 3-1; 4-8; 7-8; or 8-4. As is it shown in Fig. 3, method 1 shows the largest standard deviation of the distributions, comparing the three methods. And, as expected the standard deviation is reduced from method 1 to 2 and to 3. Method 1 has the largest standard deviation because we are: aggregating a larger heterogeneity of micro-trips; and, assuming that the distributions of trip lengths are independent for different reservoirs, which is clearly not the case.

Impact of the OD matrix on the trip lengths

To analyze the impact of the OD matrix on the trip lengths, we calculate the associated micro-trips to M^*. We investigate this impact on methods 1 and 2. The micro-trips are aggregated at the reservoir level and the average values that are calculated are listed in Table 2, for methods 1 and 2. As observed, method 1 is impacted, as shown for the cases of reservoirs 1, 2, 6 and 8. And, for method 2, the impact is observed for the cases of reservoirs: 1 to 2; 2 to 4; 2 to 5; 3 to 5; 3 to 7; 4 to 2; 4 to 6; 6 to 4; 6 to 8; and 7 to 6. Indeed, for both methods, the differences are of the order of 10 to 50 meters. But, the study network is also small. And, these differences will indeed be more significant in larger networks.

We discuss now a procedure to estimate the trip lengths based on the original calculation of micro-trips and M^*. One solution is to re-calculate the micro-trips for M^*, but this is time consuming. However for comparison, we do so for M^*.

The trip lengths for method 1, are estimated as:

$$\hat{L_k} = \frac{1}{N_k^*} \sum_i \sum_j \alpha_{ij}^* \bar{L_{ij}^k}, \forall (i,j) \in \Lambda \wedge i \neq j \tag{15}$$

where $\hat{L_k}$ is the estimated trip length for reservoir k; N_k^* is the total number of micro-trips of M^* that cross reservoir k; α_{ij}^* is the number of micro-trips of M^* that are crossing reservoir k and coming from reservoir i and going to j; $\bar{L_{ij}^k}$ is the average trip length calculated from the aggregation of all micro-trips of M that cross reservoir k. Such calculations are simple and allow to update trip lengths to dynamic variations of the OD matrix.

We aim to show based on Eq. 15 that: $\hat{L_k} \approx \bar{L^k}$. We estimate average trip length for all reservoirs based on M and M^*. The results are listed in Table 2. For a first test, we check that $\hat{L_k} = \bar{L^k}$, by setting $M = M^*$. The second test is based on M^*. As a reference for comparison,

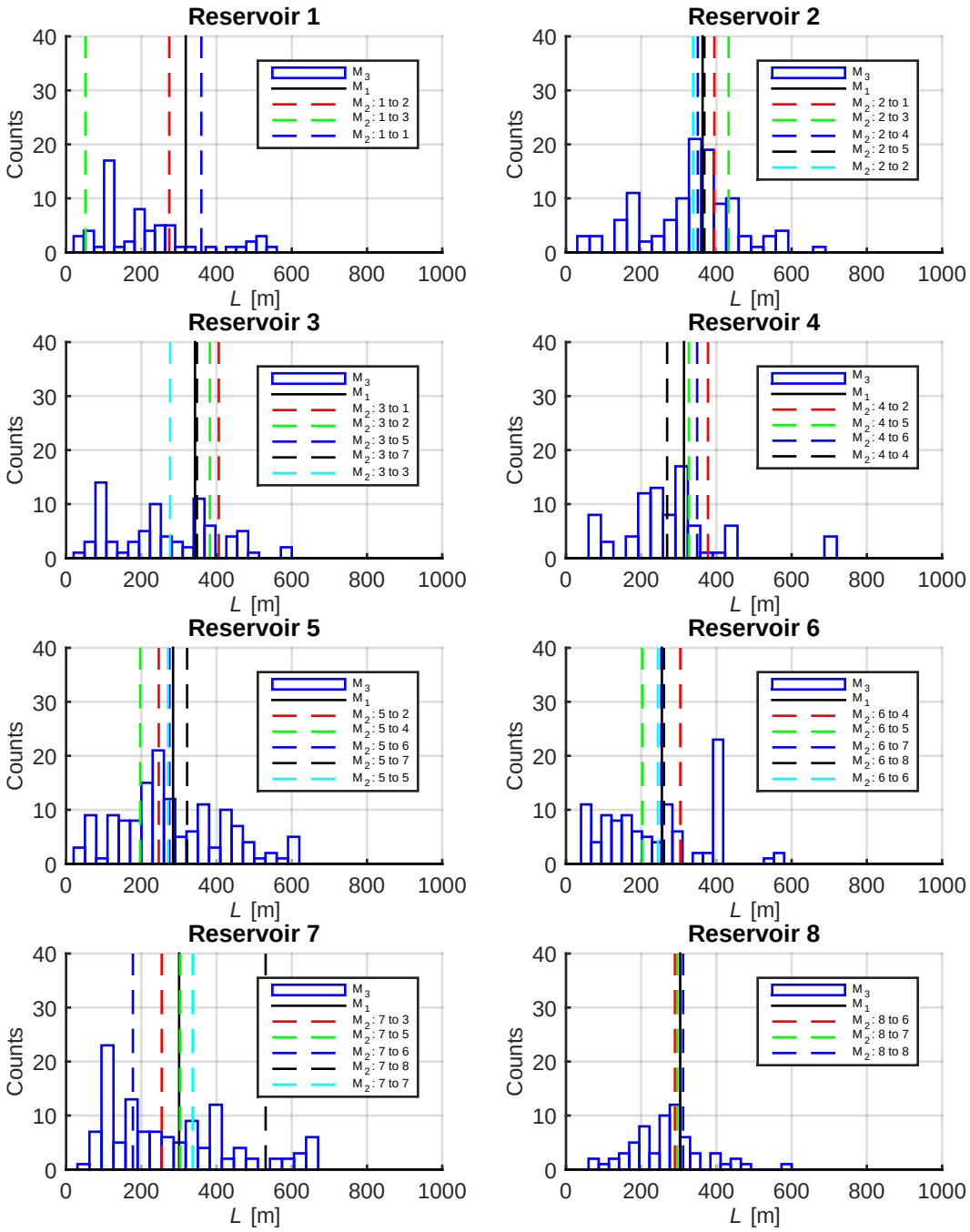

FIGURE 2 : Average trip lengths for the three methods at the reservoir level.

we sample micro-trips based on M^* and calculated the average trip lengths using method 1. The results are listed on the fourth column of Table 2. As it can be observed, the estimated average trip

lengths ($\hat{L}$) show a very good agreement with the average trip length ($\bar{L}$) calculated directly from the micro-trips aggregation. The largest absolute difference is 10 meters for reservoir 4.

For method 2, the trip lengths are estimated as:

$$\hat{L_k} = \frac{1}{N_k^*} \sum_{i}^{R} \alpha_{id}^* \bar{L_{id}^k}, \forall i \in \Lambda \wedge i \neq d \tag{16}$$

where α_{id}^* is the number of micro-trips crossing reservoir k and going to the destination adjacent reservoir d, calculated based on the new sampling; R is the number of adjacent reservoirs to k; and $\bar{L_{id}^k}$ is the average trip length calculated through method 2, considering M.

To test the estimation of average trip lengths for method 2, using Eq. 16, we consider: the OD matrices M and M^*; and the micro-trips that are sampled based on M^*. We aggregate these micro-trips according to method 2, to estimate the average trip lengths. The results are listed in Table 2. We also check that $\hat{L_k} = \bar{L^k}$, by setting $M = M^*$. The estimated average trip lengths ($\hat{L}$) show a good agreement with the ones ($\bar{L}$) calculated directly from the aggregation of the micro-trips through method 2.

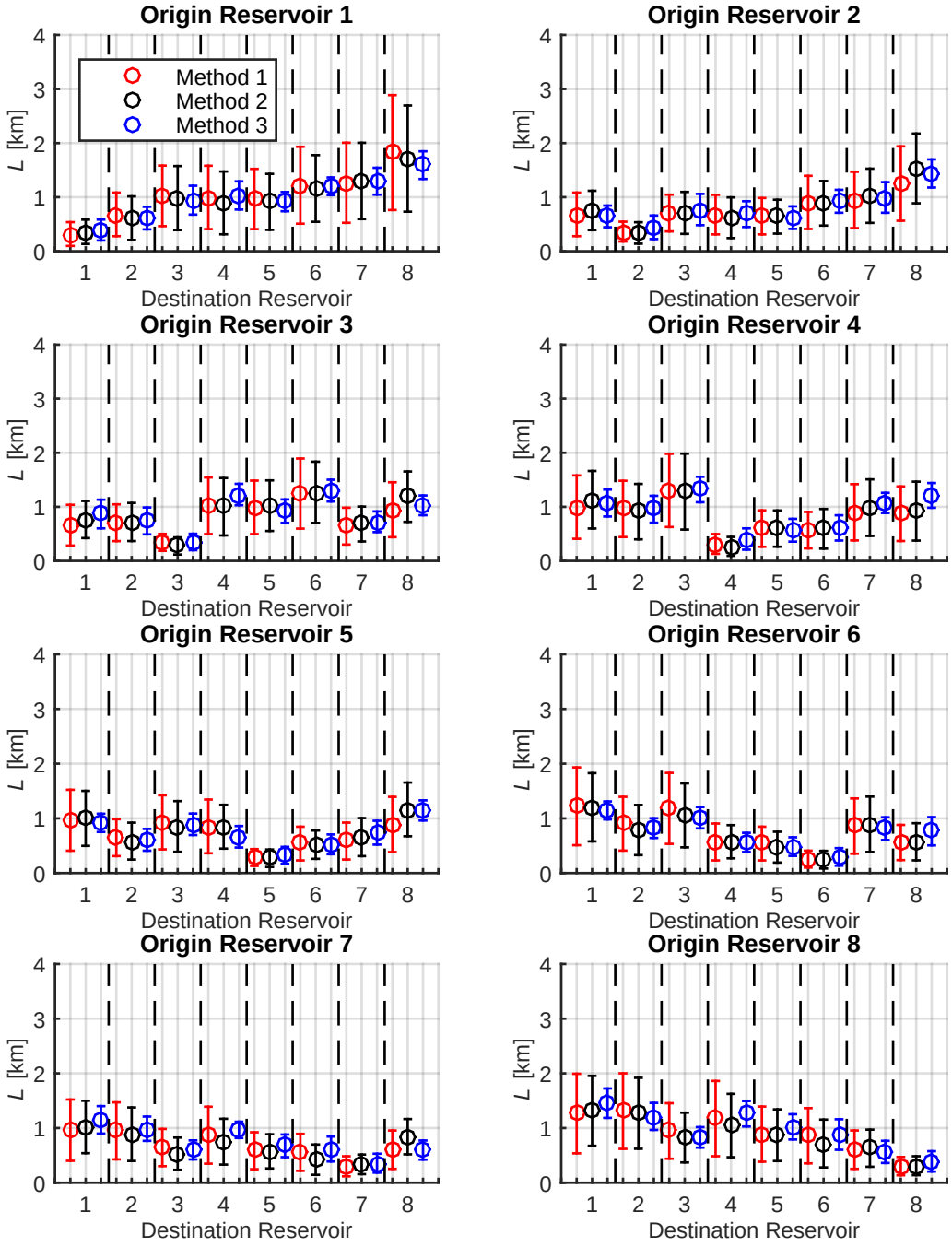

FIGURE 3 : Average and standard deviations for the most sampled macro-paths for each OD of the network. The results are calculated at the macro-path level. Each subplot correspond to an origin reservoir. The vertical dashed lines separate the different destination reservoirs.

Reservoir	M		M^*		Static		Dynamic	
	$\bar{L}$	$\hat{L}$	$\bar{L}$	$\hat{L}$	$\bar{L}$	σ_L	$\bar{L}$	σ_L
1	322	322	289	290	322	221	414	233
2	363	363	383	375	363	184	294	166
3	342	342	340	346	342	154	396	164
4	311	311	311	301	311	185	411	211
5	287	292	290	289	287	153	205	122
6	256	256	241	242	256	152	332	157
7	302	302	298	298	302	186	259	130
8	305	305	295	304	305	170	377	185

Reservoir		M		M^*		Static		Dynamic	
Origin	Destination	$\bar{L}$	$\hat{L}$	$\bar{L}$	$\hat{L}$	$\bar{L}$	σ_L	$\bar{L}$	σ_L
1	2	277	277	256	259	277	210	360	212
1	3	51	51	49	51	51	11	471	272
2	1	392	392	399	391	392	138	299	117
2	3	424	424	430	424	424	235	344	231
2	4	347	347	362	357	347	206	320	154
2	5	368	368	403	391	368	151	268	132
3	1	408	408	409	417	408	117	403	107
3	2	373	373	369	372	373	153	369	161
3	5	346	346	332	334	346	157	495	214
3	7	336	336	360	356	336	146	468	145
4	2	375	375	396	379	375	174	382	167
4	5	332	332	323	331	332	172	370	182
4	6	357	357	369	379	357	211	542	205
5	2	253	262	248	256	253	141	161	89
5	4	217	217	206	220	217	174	137	104
5	6	277	277	275	278	277	92	234	101
5	7	325	327	319	313	325	169	229	164
6	4	310	310	282	284	310	125	365	138
6	5	198	198	200	201	198	116	245	142
6	8	263	263	238	230	263	161	354	137
7	3	254	254	257	254	254	141	228	97
7	5	305	305	303	305	305	156	276	115
7	6	177	177	152	151	177	117	221	128
7	8	527	527	559	555	527	151	380	90
8	7	295	295	299	294	295	162	357	170

TABLE 2 : Average ($\bar{L}$) and estimated ($\hat{L}$) (m) trip lengths (at the reservoir level), for each reservoir and considering the two trip matrices: M; and M^*. Average ($\bar{L}$) and standard deviation (σ_L) of the trip lengths calculated based on the time-dependent micro-trips are also listed. *Top:* Method 1. *Bottom:* Method 2.

TRIP LENGTH DISTRIBUTIONS AND THE MACROSCOPIC SIMULATION

Simulation settings

For the accumulation-based macroscopic simulation, we consider the network and MFD functions shown in Fig. 1. A total simulation period of $T = 10000$ seconds is considered, discretized into intervals of $\delta t = 10$ seconds.

We consider three OD pairs: 1 to 6; 8 to 4; and 3 to 4. For each OD pair, we consider a maximum of three macro-paths. A macro-path is given by the aggregation of the micro-trips by the set of crossed reservoirs. We stress out, that a complete investigation of the macro-path definition based on the aggregation of micro-trips will be subject to a future research. For the three OD pairs, we have seven macro-paths. These macro-paths and corresponding average trip lengths calculated at the reservoir level using each method, are listed in Table 3. We consider the following demand levels. For OD 1-6, we consider the following demand levels: 0.3 (veh/s) for $\delta t \in [0, 1000]$; 1.1 (veh/s) for $\delta t \in [1000, 3000]$; and 0.2 (veh/s) for $\delta t \in [3000, 10000]$. For OF 8-4, we consider the following demand levels: 0.2 (veh/s) for $\delta t \in [0, 2000]$; 0.9 (veh/s) for $\delta t \in [2000, 4000]$; and 0.3 (veh/s) for $\delta t \in [4000, 10000]$. For OD 3-4, we consider the following demand levels: 0.2 (veh/s) $\delta t \in [0, 3000]$; 0.7 (veh/s) for $\delta t \in [3000, 5000]$; and 0.1 (veh/s) for $\delta t \in [5000, 10000]$.

The traffic flow assignment is performed using the Wardrop principle. That is, we assume that users are perfectly rational and utility minimizers. To solve the Stochastic User Equilibrium fixed point problem, we use the Method of Successive Averages (MSA). The convergence criterium of the MSA is defined by the root mean square error (RMSE):

$$RMSE = \sqrt{\sum_{O}\sum_{D}\sum_{k} \frac{(Q_k^{j+1} - Q_k^j)^2}{N}} \leq tol \tag{17}$$

where Q_k^{j+1} and Q_k^j are the new and old flows of macro-path k; N is the number of macro-paths for each OD; and tol is the convergence criterium. We set $tol = 0.01$.

Does trip length definition affect the simulated traffic states?

We investigate the influence of the three methods used to calculate the trip lengths, on the traffic states. The evolution of the accumulation and mean speed inside each reservoir is shown in Fig. 4. We observe a clear impact on the congestion pattern and duration. For methods 1 and 2, the congestion lasts between 2000 and 5000 seconds of the simulation period. Whilst, for method 3, it lasts until 8000 seconds. Indeed, different trip lengths at the reservoir level means completely different traffic states. Method 3 has a larger heterogeneity of trip lengths at the reservoir level than methods 1 and 2 (see Table 3). And, the succession of trip lengths for the same macro-path is different for the three methods. Consider, for example, the macro-path 3-2-4. For this macro-path, the trip length for reservoir 2 is: 684 meters, according to method 3; and 363 meters according to method 1. A larger trip length means a potential bottleneck (i.e., a reduction on the inflow capacity for this reservoir and specific macro-path) of this macro-path, considering method 3. Then, the congestion patterns are different for methods 1 and 3. One can also observe the evolution of the accumulation inside reservoir 2, for methods 1 and 3. The peak of the accumulation, is much larger for method 3, when compared to method 1. This is also explained by the larger heterogeneity of average trip lengths given by method 3 (see Table 3). The impact of considering a larger heterogeneity of trip lengths at the reservoir level is also discussed by Yildirimoglu and

Method 1 - Trip lengths									
Macro-path	Reservoir								N_{trips}
	1	2	3	4	5	6	7	8	
1-2-5-6	322	363	∼	∼	287	256	∼	∼	97
1-2-5-7-6	322	363	∼	∼	287	256	302	∼	48
3-2-4	∼	363	342	311	∼	∼	∼	∼	63
3-2-5-6-4	∼	363	342	311	287	256	∼	∼	46
3-2-5-7-6-4	∼	363	342	311	287	256	302	∼	13
8-7-6-4	∼	∼	∼	311	∼	256	302	305	116
8-7-3-5-2-4	∼	363	342	311	287	∼	302	305	37

Method 2 - Trip lengths								
Macro-path	Reservoir							
	1	2	3	4	5	6	7	8
1-2-5-6	277	368	∼	∼	277	245	∼	∼
1-2-5-7-6	277	368	∼	∼	325	245	177	∼
3-2-4	∼	347	373	259	∼	∼	∼	∼
3-2-5-6-4	∼	368	373	259	277	310	∼	∼
3-2-5-7-6-4	∼	368	373	259	325	310	177	∼
8-7-6-4	∼	∼	∼	259	∼	310	177	295
8-7-3-5-2-4	∼	347	346	259	253	∼	347	259

Method 3 - Trip lengths								
Macro-path	Reservoir							
	1	2	3	4	5	6	7	8
1-2-5-6	211	460	∼	∼	289	254	∼	∼
1-2-5-7-6	260	407	∼	∼	361	114	104	∼
3-2-4	∼	684	358	185	∼	∼	∼	∼
3-2-5-6-4	∼	416	335	206	267	260	∼	∼
3-2-5-7-6-4	∼	75	304	258	248	411	104	∼
8-7-6-4	∼	∼	∼	296	∼	411	299	275
8-7-3-5-2-4	∼	403	467	101	215	∼	182	300

TABLE 3 : Average trip lengths (m) at the reservoir level, for the seven macro-paths considered for the accumulation-based simulation. *Top:* Method 1. The number of micro-trips that define each macro-path is also listed. *Middle:* Method 2. *Bottom:* Method 3.

Geroliminis (*3*).

Despite at the macro-path level, the three methods yield similar average trip lengths, the succession of trip lengths for the macro-paths calculated by the three methods have a clear impact on the traffic states inside each reservoir.

In order to highlight which method is more realistic, a comparison with a trip-based simula-

tion, where vehicles follow the same trip sequence with the estimated micro-trips, will be discussed in the extended version of this paper. This aims to put in evidence the importance of variable trip lengths versus average trip lengths assumption, for different trips inside the same reservoir.

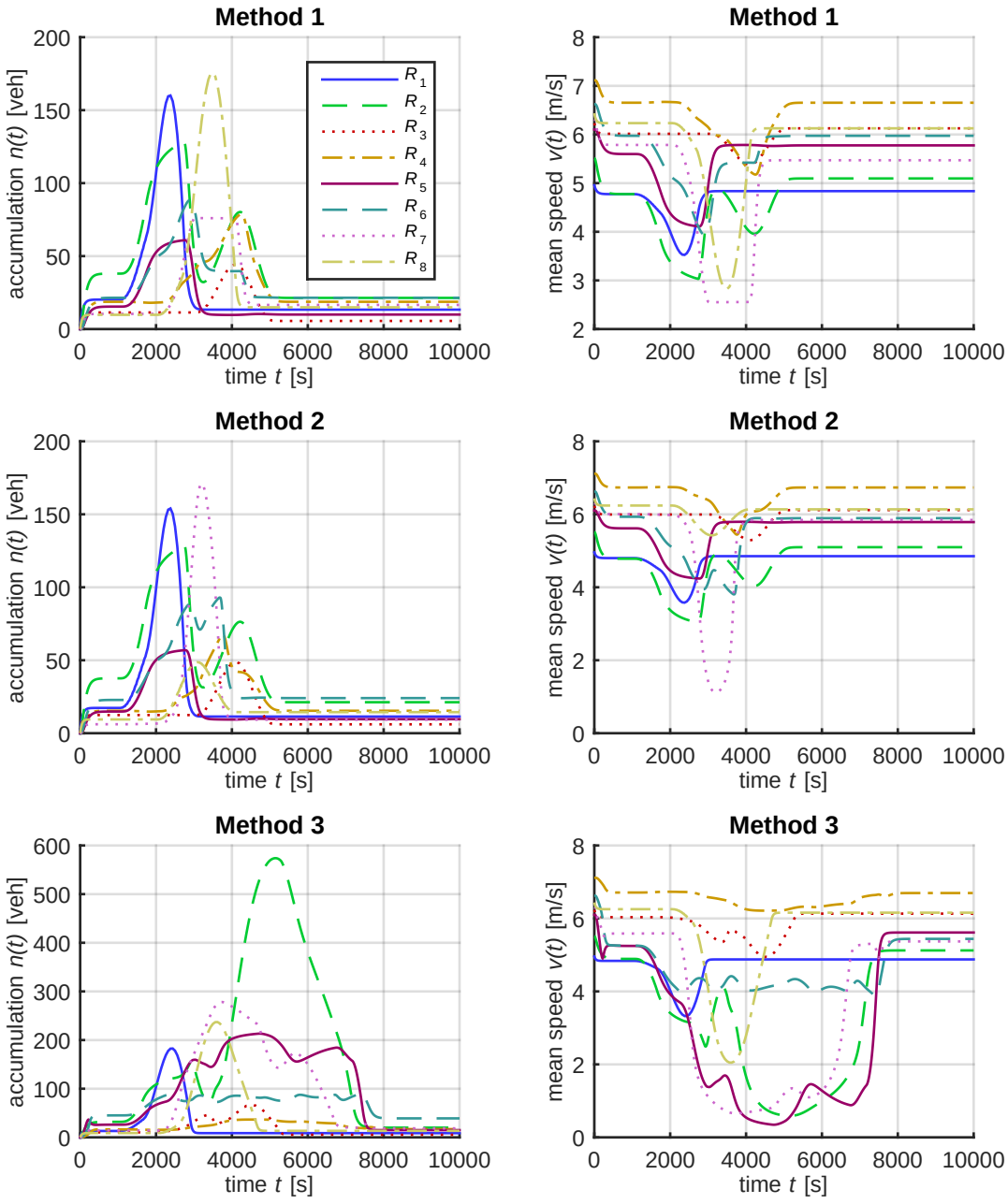

FIGURE 4 : Evolution of *n(t)* and *v(t)* during the simulation period, considering the three methods to calculate the trip lengths.

Are the trip length distributions congestion dependent?

For now, the trip lengths were calculated based on shortest-paths in distance on the microscopic network, without considering travel times and thus traffic states. Hereby, we investigate the dependence of the trip lengths on the traffic states. For this purpose, we calculate time-dependent micro-trips, based on the mean speed given by the MFD dynamics. We consider the evolution of the mean speed, for Method 3 (Fig. 4), between 2000 and 8000 seconds. Based on this, we estimate an average mean speed for each reservoir. Considering the latter and the link lengths of the microscopic network, we calculate time-dependent micro-trips based on the same microscopic od pairs of the micro-trips listed in Ξ. We recover the microscopic lengths of these micro-trips and aggregate them according to the three methods the reservoir level. We then compare these results against the static trip lengths, calculated based on Ξ. For the comparison at the reservoir level, we define a parameter α that defines the absolute difference between the dynamic ($\overline{L_d}$) and static ($\overline{L_s}$) average trip lengths, as:

$$\alpha = \overline{L_d} - \overline{L_s} \tag{18}$$

The static ($\overline{L_s}$) and dynamic ($\overline{L_d}$) average trip lengths and corresponding standard deviations are listed on Table 2, for methods 1 and 2. The absolute differences defined by α for the three methods, at the reservoir level, is shown in Fig. 5. As a reference for method 3, we consider the set of macro-paths Ψ. The histograms represent the relative differences of trip lengths, for the same macro-path, defined at the reservoir level.

As observed in Table 2, the average trip lengths at the reservoir level are affected by $\sim$ 100 meters for method 1 and 2. There are a few exceptions. Consider as an example, the case of method 2 for micro-trips going from reservoir 1 to 3. At the static level, there are only 13 micro-trips that are aggregated, while for the dynamic one there are 635 micro-trips. In fact, performing the static sampling, micro-trips that departure from nodes close to the border between reservoirs 1 and 3 are more probable to cross to reservoir 3 rather than 2. However, when reservoir 2 is congested, the link costs increase and consequently micro-trips that begin in nodes that are more far away from the border between reservoirs 1 and 3, will more probably cross it. On the other hand, the static micro-trips are not sensible to the reservoir definition. While in the dynamic case, we are considering the mean speed calculated through the MFD simulation and this induces also a dependence of the macroscopic network. Thus, the number of micro-trips that are aggregated to calculate the dynamic trip lengths is different. Method 3 is the more sensible to the number of aggregated micro-trips (Fig. 5). For this consider, as example, macro-path 1-3. The set of corresponding average trip lengths (in meters) are: 47 (reservoir 1) and 434 (reservoir 3) meters with 6 micro-trips associated, for the static case; and, 535 (reservoir 1) and 471 (reservoir 3) meters with 116 micro-trips associated, for the dynamic case. The latter also highlights the reasons previously mentioned. And, for this particular case, the difference between the static and dynamic cases are also due to the special geometry of the macroscopic network. Note that, there are only two connecting nodes between reservoirs 1 and 3 (Fig. 1).

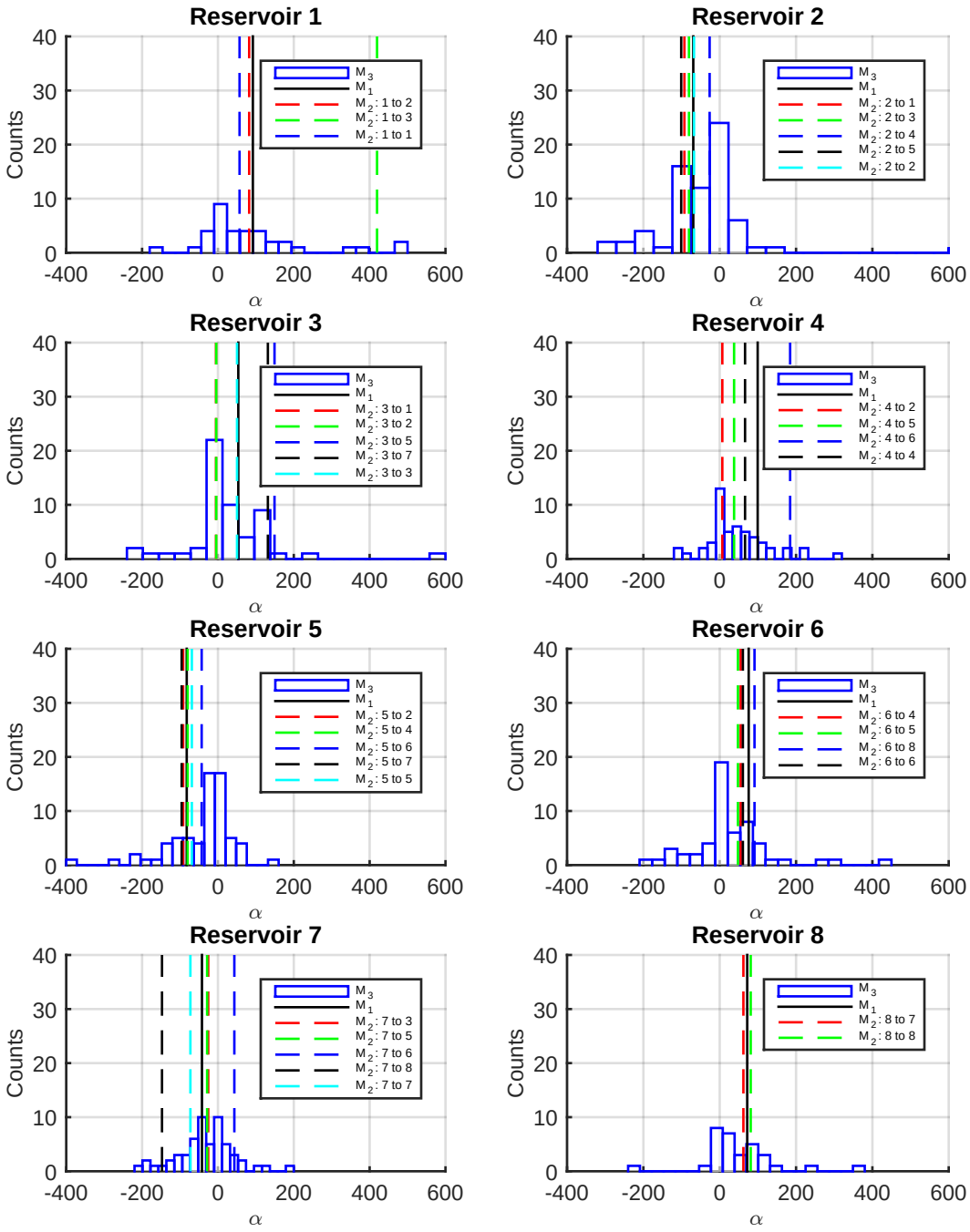

FIGURE 5 : Absolute difference α (km) at the reservoir level, between the trip lengths calculated based on the time-dependent micro-trips and the micro-trips listed on Ξ.

CONCLUSIONS

In this paper, we discuss three methods to calculate macroscopic trip lengths at both the reservoir and macro-path levels. These methods are based on the aggregation of micro-trips. We show that the different methods give different average trip lengths at the reservoir level. And, this has a significant impact on the macroscopic simulation. A trip-based simulation considering variable versus average trip lengths inside the same reservoir will be presented in the extended version of the paper, to put in evidence the importance of more refined definitions of trip lengths for the macroscopic simulation. Different trip lengths at the reservoir level yield completely different traffic dynamics. At the macro-path level, the impact of the different methods is on the standard deviation and not on the average of the trip lengths. We show that the trip lengths are congestion-dependent at the reservoir level. Method 3 is the more sensible to congestion, at the reservoir level. We also show the dependence of the trip lengths on the OD matrix. And, we discuss a procedure to quickly estimate the trip lengths based on a new definition of the OD matrix, without the need to recalculate the micro-trips. This is very useful when OD matrix is changing with time. We show that this procedure gives coherent average trip lengths for methods 1 and 2, compared to when we recalculate the micro-trips.

As future research directions, we plan to investigate the dependence of the trip lengths on: the number of micro-trips N_{trips}; and on the algorithm used to calculate the micro-trips. A ground-truth validation of these methods is also foreseen. We also plan to further tackle the question of the macro-path definition, based on the micro-trips aggregation.

ACKNOWLEDGEMENTS

This project is supported by the European Research Council (ERC) under the European Union's Horizon 2020 research and innovation programme (grant agreement No 646592 - MAGnUM project). S. F. A. Batista also acknowledges funding support by the region Auvergne-Rhône-Alpes (ARC7 Research Program) and from the University of Lyon supported by the PALSE mobility program.

References

[1] Daganzo, C., Urban gridlock: Macroscopic modeling and mitigation approaches. *Transportation Research Part B: Methodological*, Vol. 41, 2007, p. 4962.

[2] Geroliminis, N. and C. Daganzo, Existence of urban-scale macroscopic fundamental diagrams: Some experimental findings. *Transportation Research Part B: Methodological*, Vol. 42, 2008, pp. 759–770.

[3] Yildirimoglu, M. and N. Geroliminis, Approximating dynamic equilibrium conditions with macroscopic fundamental diagrams. *Transportation Research Part B: Methodological*, Vol. 70, 2014, pp. 186–200.

[4] Ramezani, M., J. Haddad, and N. Geroliminis, Dynamics of heterogeneity in urban networks: aggregated traffic modeling and hierarchical control. *Transportation Research Part B*, Vol. 74, 2015, pp. 1–19.

[5] Godfrey, J. W., The mechanism of a road network. *Traffic Engineering and Control*, Vol. 11, 1969, pp. 323–327.

[6] Buisson, C. and C. Ladier, Exploring the Impact of Homogeneity of Traffic Measurements on the Existence of Macroscopic Fundamental Diagrams. *Transportation Research Record Journal of the Transportation Research Board*, Vol. 2124, 2009.

[7] Ambühl, L. and M. Menendez, Data fusion algorithm for macroscopic fundamental diagram estimation. *Transportation Research Part C: Emerging Technologies*, Vol. 71, 2016, pp. 184–197.

[8] Derrman, T., R. Frank, and F. Viti, Towards Estimating Urban Macroscopic Fundamental Diagrams From Mobile Phone Signaling Data: A Simulation Study. In *Transportation Research Board 96th Annual Meeting*, Washington DC, USA, 2017.

[9] Lodera, A., L. Ambühl, M. Menendez, and K. W. Axhausen, Data fusion algorithm for macroscopic fundamental diagram estimation. *Transportation Research Part C: Emerging Technologies*, Vol. 82, 2017, pp. 88–101.

[10] Haddad, J. and N. Geroliminis, On the stability of traffic perimeter control in two-region urban cities. *Transportation Research Part B: Methodological*, Vol. 46, 2012, p. 11591176.

[11] Ekbatani, M., M. Papageorgiou, and I. Papamichail, Urban congestion gating control based on reduced operational network fundamental diagrams. *Transportation Research Part C: Emerging Technologies*, Vol. 33, 2013, pp. 74–87.

[12] Haddad, J., Optimal perimeter control synthesis for two urban regions with aggregate boundary queue dynamics. *Transportation Research Part B: Methodological*, Vol. 96, 2017, pp. 1–25.

[13] Arnott, R., A bathtub model of downtown traffic congestion. *Journal of Urban Economics*, Vol. 76, 2013, pp. 110–121.

[14] Leclercq, L., C. Parzani, V. L. Knoop, J. Amourette, and S. Hoogendoorn, Macroscopic traffic dynamics with heterogeneous route patterns. *Transportation Research Part C*, Vol. 59, 2015, pp. 292–307.

[15] Fosgerau, M., Congestion in the bathtub. *Economics of Transportation*, Vol. 4, 2015, pp. 241–255.

[16] Lamotte, R. and N. Geroliminis, The morning commute in urban areas: Insights from theory and simulation. In *Transportation Research Board 95th Annual Meeting.*, 2016, pp. 16–2003.

[17] Leclercq, L., A. Sénécat, and G. Mariotte, Dynamic macroscopic simulation of on-street parking search: A trip-based approach. *Transportation Research Part B: Methodological*,

Vol. 101, 2017, pp. 268–282.
[18] Mariotte, G., L. Leclercq, and S. F. A. Batista, *A trip-based multi-reservoir MFD simulation framework*, 2017.
[19] Gayah, V. V. and C. F. Dagamzo, Clockwise hysteresis loops in the Macroscopic Fundamental Diagram: An effect of network instability. *Transportation Research Part B: Methodological*, Vol. 45, 2011, pp. 643–655.
[20] Frejinger, E., M. Bierlaire, and M. Ben-Akiva, Sampling of alternatives for route choice modeling. *Transportation Research Part B*, Vol. 43, 2009, pp. 984–994.
[21] Flotterod, G. and Bierlaire, Metropolis-Hastings sampling of paths. *Transportation Research Part B*, Vol. 48, 2013, pp. 53–66.
[22] Leclercq, L., Hybrid approaches to the solutions of the "Lighthill-Whitham-Richards" model. *Transportation Research Part B: Methodological*, Vol. 41, 2007, pp. 701–709.
[23] Cabrera Delgado, J. and P. Bonnel, Level of aggregation of zoning and temporal transferability of the gravity distribution model: The case of Lyon. *Journal of Transport Geography*, Vol. 51, 2016, pp. 17–26.